Toxicology and Applied Pharmacology 257 (2011) 242–249

Contents lists available at SciVerse ScienceDirect

Toxicology and Applied Pharmacology

journal homepage: www.elsevier.com/locate/ytaap

# Cardiac toxicity of 5-ring polycyclic aromatic hydrocarbons is differentially dependent on the aryl hydrocarbon receptor 2 isoform during zebrafish development

John P. Incardona *, Tiffany L. Linbo, Nathaniel L. Scholz

*Ecotoxicology and Environmental Fish Health Program, Environmental Conservation Division, Northwest Fisheries Science Center, 2725 Montlake Blvd E, Seattle, Washington 98112, United States*

ARTICLE INFO

*Article history:*
Received 6 May 2011
Revised 8 September 2011
Accepted 8 September 2011
Available online 19 September 2011

*Keywords:*
Polyaromatic compounds
Non-point source pollution
Fish embryogenesis, heart development
Metabolism

ABSTRACT

Petroleum-derived compounds, including polycyclic aromatic hydrocarbons (PAHs), commonly occur as complex mixtures in the environment. Recent studies using the zebrafish experimental model have shown that PAHs are toxic to the embryonic cardiovascular system, and that the severity and nature of this developmental cardiotoxicity varies by individual PAH. In the present study we characterize the toxicity of the relatively higher molecular weight 5-ring PAHs benzo[a]pyrene (BaP), benzo[e]pyrene (BeP), and benzo[k]fluoranthene (BkF). While all three compounds target the cardiovascular system, the underlying role of the ligand-activated aryl hydrocarbon receptor (AHR2) and the tissue-specific induction of the cytochrome p450 metabolic pathway (CYP1A) were distinct for each. BaP exposure (40 μM) produced AHR2-dependent bradycardia, pericardial edema, and myocardial CYP1A immunofluorescence. By contrast, BkF exposure (4–40 μM) caused more severe pericardial edema, looping defects, and erythrocyte regurgitation through the atrioventricular valve that were AHR2-independent (i.e., absent myocardial or endocardial CYP1A induction). Lastly, exposure to BeP (40 μM) yielded a low level of CYP1A+ signal in the vascular endothelium of the head and trunk, without evident toxic effects on cardiac function or morphogenesis. Combined with earlier work on 3- and 4-ring PAHs, our findings provide a more complete picture of how individual PAHs may drive the cardiotoxicity of mixtures in which they predominate. This will improve toxic injury assessments and risk assessments for wild fish populations that spawn in habitats altered by overlapping petroleum-related human impacts such as oil spills, urban stormwater runoff, or sediments contaminated by legacy industrial activities.

Published by Elsevier Inc.

## Introduction

Polycyclic aromatic hydrocarbons are ubiquitous pollutants derived from fossil fuels that virtually always occur in complex mixtures. The most commonly measured PAHs are compounds containing 2 to 6 benzene rings. Mixtures derived from petroleum sources (i.e., petrogenic) are dominated by compounds with 2 to 4 rings, while mixtures derived from combustive sources (i.e., pyrogenic) or products such as creosote or coal tar have proportionally higher concentrations of compounds with 4 to 6 rings. Consistent with predominantly pyrogenic inputs in land-based stormwater runoff, aquatic sediments in urbanized areas are often dominated by 4- to 6-ring compounds (Kimbrough and Dickhut, 2006; Stein et al., 2006). Fish early life history stages are important sentinels for PAH toxicity in the environment because fish embryos and larvae are highly sensitive to PAHs from a variety of sources, including crude oil spills, creosote wood preservatives, oil sands, and sediments impacted by urban runoff (Carls et al., 1999; Colavecchia et al., 2004; Couillard, 2002; Heintz et al., 1999, 2000; Sundberg et al., 2005; Vines et al., 2000). Exposure to petrogenic and pyrogenic PAH mixtures produces toxicity syndromes with overlapping characteristics that primarily involve the cardiovascular system (Billiard et al., 2008; Incardona et al., 2011). To better understand the toxicity of complex PAH mixtures, we initiated a series of studies of individual PAH toxicities using the zebrafish model (Incardona et al., 2004, 2005, 2006). These previous studies focused on compounds with 2 rings (naphthalene), 3 rings (fluorene, dibenzothiophene, phenanthrene, anthracene), and 4 rings (pyrene, benz[a]anthracene, benz[b]anthracene, chrysene).

Among these compounds, a few lack any overt embryotoxicity in zebrafish, including naphthalene, anthracene, and chrysene (Incardona et al., 2004). Others, however, produce distinct functional and morphological defects at different developmental stages. A major focus in recent years has been a determination of the role of the aryl hydrocarbon (AHR)/cytochrome P4501A (CYP1A) pathway in the toxicity of different PAHs. PAHs induce their own metabolism by activating transcription of *cyp1a* genes through AHR binding (Nebert et al., 2004), but they also have the potential to cause AHR-dependent toxicity in the same manner as dioxins (Carney et al., 2004). Previous studies using PAH parent compounds, other naturally occurring PAHs, or PAH-like model compounds have identified at least three major

* Corresponding author at: Environmental Conservation Division, Northwest Fisheries Science Center, National Oceanic and Atmospheric Administration, 2725 Montlake Blvd E., Seattle, WA 98112, United States. Fax: +1 206 860 3335.
*E-mail address:* john.incardona@noaa.gov (J.P. Incardona).

0041-008X/$ – see front matter. Published by Elsevier Inc.
doi:10.1016/j.taap.2011.09.010

modes of PAH toxicity: AHR-independent effects on cardiac rate and rhythm (Incardona et al., 2004, 2005, 2009), AHR-dependent impacts on cardiac morphogenesis (Billiard et al., 2006; Clark et al., 2010; Incardona et al., 2006; Scott et al., 2011), and toxicity dependent on CYP1A metabolism (Incardona et al., 2006). To build on this improved understanding for lower molecular weight PAHs, in the present study we investigate modes of toxic action for the 5-ring compounds benzo[a]pyrene (BaP), benzo[e]pyrene (BeP), and benzo[k]fluoranthene (BkF). We used the same approach as in our past studies, testing high concentrations of PAHs that lead to robust and reproducible toxic effects in zebrafish embryos. This approach is not intended to be environmentally realistic, but allows detection of toxic mechanisms that could potentially lead to impacts in more sensitive species under field conditions.

BaP, BeP, and BkF are all relatively potent CYP1A inducers in fish (Barron et al., 2004), and might therefore be expected to cause AHR-dependent cardiotoxicity similar to that previously described for benz[a]anthracene (BaA (Incardona et al., 2006)) and retene (Scott et al., 2011). The AHR pathway is more complicated in fish than in mammals due to gene and genome duplication (Hahn, 2002). Zebrafish have three AHR orthologs, AHR1A, AHR1B, and AHR2 (Andreasen et al., 2002a; Karchner et al., 2005; Tanguay et al., 1999). Although not yet definitively determined, these orthologs are likely to subserve tissue- or developmental stage-specific functions. So far, only AHR2 has been found to play a role in canonical dioxin-like toxicity (Andreasen et al., 2002b; Henry et al., 1997), which in zebrafish embryos manifests primarily as defects in late steps of cardiac morphogenesis occurring around 48 hours post fertilization (hpf) (Antkiewicz et al., 2005). BaA cardiotoxicity in zebrafish is prevented by morpholino knockdown of AHR2, and BkF causes cardiotoxicity in *Fundulus heteroclitus* embryos that is dependent on that species' AHR2 isoform (Clark et al., 2010). As we have observed for a number of other PAHs, here we describe distinct tissue-specific patterns of CYP1A induction and toxicity differentially dependent on zebrafish AHR2 for BaP, BeP, and BkF.

## Materials and methods

*Chemicals.* Benzo[*a*]pyrene (>99% purity), benzo[*e*]pyrene (99% purity), and benzo[*k*]fluoranthene (98% purity), and MS-222 were obtained from Sigma-Aldrich, St. Louis, MO. Stock PAH solutions were made in dimethyl sulfoxide (DMSO, tissue culture grade, Sigma) at 10 mg/ml. Final concentrations of DMSO were 0.1% or lower in exposure medium.

*Zebrafish exposures.* Zebrafish wild type AB strain and the Tg(*fli1*-EGFP) line (Lawson and Weinstein, 2002) were maintained and spawned as detailed elsewhere (Linbo, 2009). Fish were treated according to an animal care committee-approved protocol and anesthetized with ~1 mM MS-222 when necessary. Static exposures were carried out in glass 60-mm Petri dishes, with 15–25 embryos in 10 mL. Depending on the number of morpholino-injected embryos, some assays had 15–20 or 20–25 embryos per dish. In initial exposures, each treatment was performed with two technical replicates. Morpholino experiments generally used one dish per treatment, and entire experiments were replicated rather than having technical replicates within treatments. In these studies, individual embryos are the more important replicate unit. The small mass of zebrafish embryos (~1 mg wet weight) would not be expected to influence toxicokinetics at the concentrations tested. All exposures used doses above the solubility limit of the compounds, which is 9 μM for BaP, 25 μM for BeP, and 3 μM for BkF. Initial tests utilized 40 μM for each BaP, BeP, and BkF, while binary mixtures included 20 μM of each compound, and the ternary mixture included 13 μM of each. Previous studies have shown that dose-dependent responses for PAHs can be obtained above a compound's solubility limit in small volume static exposures, probably due to complex kinetics between dissolution, adsorption to the vessel wall, and vaporization (Incardona et al., 2004, 2005, 2006).

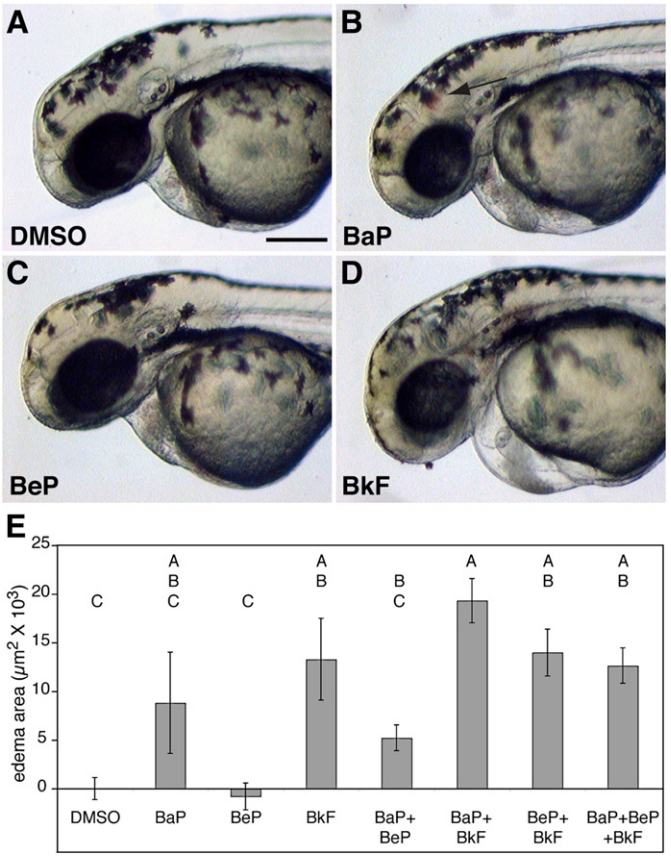


**Fig. 1.** Differential occurrence of pericardial edema associated with exposure to 5-ring PAHs. Embryos were exposed to each compound at 40 μM from 4 to 48 hpf, then imaged and scored for pericardial edema. Binary and tertiary mixtures included 20 μM and 13.3 μM each compound, respectively (40 μM total PAH). Representative images are shown for control (DMSO-exposed, A), BaP (B), BeP (C), and BkF (D). (E) Increased pericardial area (mean ± s.e.m.) was quantified as described in Materials and methods from images of at least 15 embryos per treatment group. Letters *A, B, C* indicate statistically similar groups determined by Dunnett's Method (α=0.05). Intracranial hemorrhage indicated by arrow in (B). Scale bar is 200 μm.

*Morpholino injections.* Morpholino oligonucleotides (GeneTools, Philomath, OR) included translation-blocking morpholinos targeting zebrafish AHR2 (5′-TGTACCGATACCCGCCGACATGGTT-3′, *ahr2*-MO), CYP1A (5′-TGGATACTTTCCAGTTCTCAGCTCT-3′, *cyp1a*-MO) (Teraoka et al., 2003), and negative control morpholinos included mismatched oligonucleotide for AHR2 (5′-TGaACCcATACCCGCCGtCATcGTT-3′, 4Mis-*ahr2*-MO) and a generic "standard control" (5′-CCTCTT ACCTCAGTTACAATTTATA-3′, std-MO). Embryos were injected at the 1–4 cell stage (0.25–1 hpf) with a maximum volume of 4 nL morpholino solution (100 μM) using a PLI90 Picoinjector (Harvard

**Table 1**
Effects of BaP and BkF on cardiac function at 48 hpf.

| Cardiac parameter | DMSO | BaP | BkF |
|---|---|---|---|
| Heart rate (beats/min) | 128 ± 2 | 120 ± 3* | 93 ± 2* |
| Atrial diameter (μm) | 84.1 ± 2.0 | 82.9 ± 3.5 | 99.6 ± 5.6 * |
| Atrial fractional shortening (%) | 21.7 ± 2.1 | 23.7 ± 1.5 | 27.3 ± 1.3* |
| Atrial stroke volume ($mm^3 \times 10^{-3}$) | 2.6 ± 0.3 | ND | 4.5 ± 0.5 |
| Atrial ejection fraction (%) | 45.8 ± 3.6 | ND | 45.9 ± 3.1 |
| Ventricular diameter (μm) | 87.1 ± 1.8 | 85.1 ± 2.9 | 92.3 ± 5.5 |
| Ventricular fractional shortening (%) | 22.9 ± 1.9 | 19.5 ± 1.7 | 23.1 ± 2.4 |
| Ventricular stroke volume ($mm^3 \times 10^{-3}$) | 3.0 ± 0.5 | ND | 2.8 ± 0.2 |
| Ventricular ejection fraction (%) | 47.1 ± 1.5 | ND | 50.4 ± 4.0 |
| Cardiac output ($mm^3$/min) | 0.36 | ND | 0.28 |

Values are mean ± s.e.m.; $N = 12$ for heart rate, $N = 10$ for all other measures.
*Statistically different from DMSO at $p < 0.05$, Dunnett's Method post-hoc to one-way ANOVA.

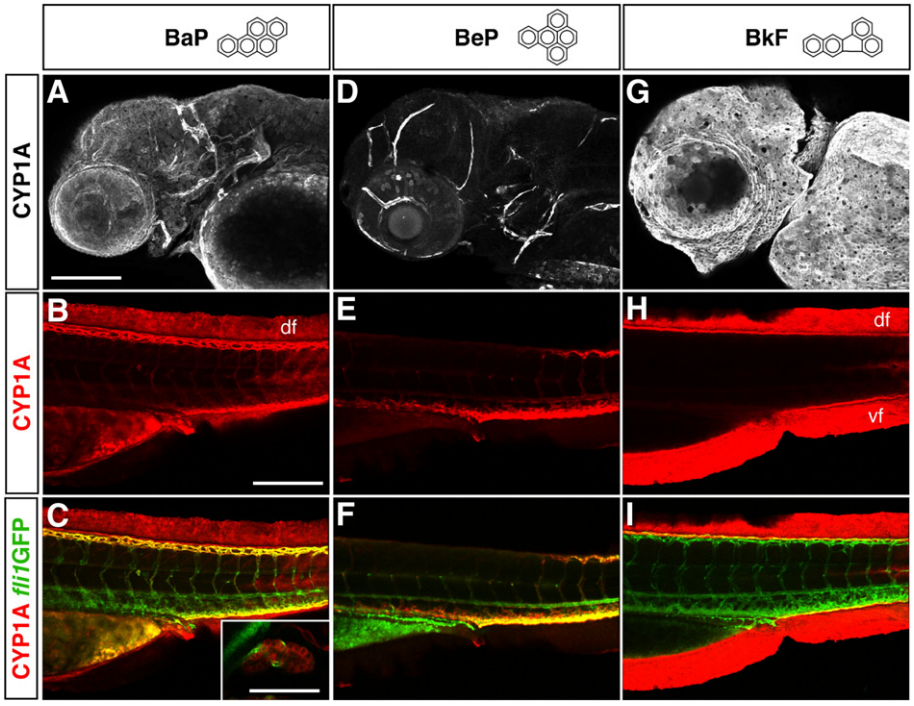


**Fig. 2.** Tissue-specific CYP1A induction following exposure to BaP, BeP, or BkF. Embryos expressing *fli1*-GFP were exposed to BaP (A-C), BeP (D-F) or BkF (G-I) from 4 to 72 hpf, fixed and processed for CYP1A and GFP immunofluorescence as described in the Materials and methods. Lateral confocal stack projection views of the head region are shown with CYP1A immunofluorescence in grayscale (A, D, G). Confocal optical sections of trunk are shown in B, C, E, F, H, and I, with CYP1A in red and vascular (*fli1*-driven) GFP in green. Co-localization of CYP1A in $GFP^+$ vascular endothelial cells is seen as yellow. Inset (C) shows CYP1A immunofluorescence in liver bud. *df*, dorsal finfold; *vf*, ventral finfold. Scale bars are 200 μm (A–I) and 50 μm (inset, C).

Apparatus, Holliston, MA). Injection volume was calculated after measuring the diameter of a droplet injected into heavy oil. Injected embryos were allowed to recover in system water at 28.5 °C to 50% epiboly (5–6 h) before use in exposure studies. For fluorescein- or rhodamine-conjugated morpholinos (*cyp1a*-MO and std-MO), embryos were selected for use in exposures on an epifluorescent stereoscope based on fluorescence intensity and an even distribution in blastomeres. Based on assessment of tagged morpholinos, injection efficiencies were determined to be >95%. Therefore, the number of embryos unsuccessfully injected with the untagged *ahr2*-MO would have little impact to the overall assay. This was confirmed by positive control experiments with BaA.

*Imaging of live embryos/larvae and measurements of cardiac function.* Digital still micrographs were obtained and videomicroscopy of live embryos and larvae performed as described previously (Incardona et al., 2004, 2006). Image J (http://rsbweb.nih.gov/ij/) was used for all measurements except heart rate, which was counted in unanesthetized animals over a 15-s interval. To quantify the degree of pericardial edema, lateral images were obtained for at least 14 embryos or larvae mounted in 3% methylcellulose, and the pericardial area measured in pixels by tracing the boundaries of the pericardial space. Pixel area was converted to $\mu m^2$ based on the calibrated magnification. To obtain an "edema area", the mean area in uninjected DMSO-exposed control embryos (i.e. no edema) was subtracted from individual measurements to give an estimate of the degree of pericardial edema (i.e. increase of pericardial area above control). Contractility was assessed by measuring fractional shortening, an indicator of systolic contractility normalized to chamber diameter (Bendig et al., 2006). End-diastolic and end-systolic diameters of the atrium were measured in digital video frames, and fractional shortening calculated as (end-diastolic diameter) − (end-systolic diameter)/(end-diastolic diameter)*100. For stroke volume, the end-diastolic and end-systolic perimeters of each chamber were traced and the major and minor axes extracted and used to calculate the chamber volume with the formula for a prolate spheroid ($4/3\pi * a * b^2$) (Kopp et al., 2005). After converting from pixels to $mm^3$, stroke volume was calculated as end-diastolic volume−end-systolic volume, ejection fraction as stroke volume/end-diastolic volume, and cardiac output as stroke volume*heart rate.

*Immunofluorescence and confocal microscopy.* Antibodies used for immunofluorescence were anti-fish CYP1A mouse monoclonal C10-7 (Myers et al., 1993) (Cayman Chemical, Ann Arbor, MI), anti-myosin heavy chain monoclonal MF20 (Bader et al., 1982) (Developmental Studies Hybridoma Bank, University of Iowa), and AlexaFluor488-conjugated monoclonal anti-GFP (Invitrogen). Embryos were fixed 3 h to overnight in 4% phosphate-buffered paraformaldehyde, and processed for immunofluorescence as described previously (Incardona et al., 2004, 2005). Secondary antibodies (Invitrogen-Molecular Probes, Eugene, OR) were AlexaFluor488- or AlexaFluor568-conjugated goat-anti-mouse IgG3 (mAb C10-7) and AlexaFluor568-conjugated goat anti-mouse IgG2b (MF20). Immunolabeled embryos were mounted in 3% methylcellulose and imaged using a Zeiss LSM 5 Pascal confocal system with Ar and HeNe lasers.

*Statistical analysis.* Statistics were performed with JMP 6.0.2 for Macintosh (SAS Institute, Cary, NC). For heart measures (edema and functional parameters), each dataset was analyzed by 1-way ANOVA with treatment as the independent variable. If the ANOVA showed a significant effect of treatment ($p<0.05$), treatment group means were compared in post-hoc tests with either Dunnett's Method or Tukey–Kramer Honestly Significant Differences test ($\alpha=0.05$). Effects of morpholino injection were determined by including both uninjected and control-MO injected groups in the statistical analysis.

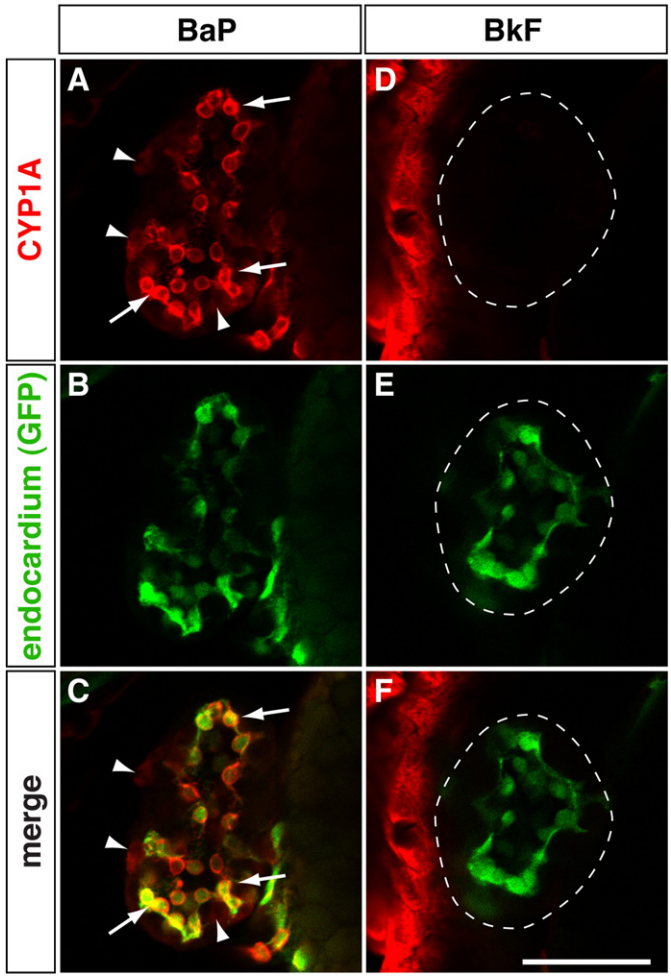


**Fig. 3.** Exposure to BaP but not BkF results in myocardial and endocardial CYP1A induction. Embryos expressing *fli1*-GFP were exposed to BaP (A–C), or BkF (D–F) from 4 to 72 hpf, fixed and processed for CYP1A (A, D; red) and GFP (B, E; green) immunofluorescence as described in the Materials and methods. Arrowheads and arrows indicate CYP1A$^+$ myocardial cells and endocardial cells, respectively. Co-localization of CYP1A and GFP is seen as yellow in the merged image. Dashed line marks the outline of the myocardium in the BkF-exposed embryo. Scale bar is 50 μm.

## Results

### *Benzo[a]pyrene and benzo[k]fluoranthene exposure results in distinct cardiac defects*

After incubation through 48 hpf, pericardial edema was observed in an average of 38 ± 4% (± s.e.m., $N = 41$, 2 replicates) of embryos exposed to 40 μM BaP and 84 ± 11% ($N = 42$, 2 replicates) of embryos exposed to 40 μM BkF. Embryos exposed to BeP appeared no different than controls. The severity of pericardial edema associated with exposure to each compound was quantified by measuring the pericardial area in lateral images (Fig. 1). In general, BkF exposure resulted in more severe edema, a greater reduction in cardiac function, and more severe impacts on late stages of cardiac morphogenesis. By 48 hpf, approximately 10% of BkF-exposed embryos had severe looping defects, and a third showed regurgitation of erythrocytes through the atrioventricular valve (Movie S1). In contrast, BaP-exposed embryos showed only mild looping defects and no regurgitation. Measurement of several cardiac functional parameters also indicated that the effects of BaP and BkF were distinct (Table 1). At 48 hpf BaP-exposed embryos showed a mild but statistically significant bradycardia (120 beats/min vs. 128 in controls, $p = 0.03$; ANOVA and Dunnett's post-hoc), while BkF-exposed embryos showed a more severe bradycardia (93 beats/min, $p < 0.0001$). Measurement of chamber dimensions showed that the atrial chambers were dilated in BkF-exposed embryos, with a mean diameter of 99.6 ± 5.6 μm compared to controls at 84.1 ± 2.0 μm ($p = 0.02$; ANOVA and Dunnett's post-hoc). A quantitative analysis of contractility showed an elevation of atrial fractional shortening from 21.7 ± 2.1% in controls to 27.3 ± 1.3% ($p = 0.04$; ANOVA and Dunnett's post-hoc) in BkF-exposed embryos, but no change in ejection fraction. The stroke volume was elevated from 0.0026 $mm^3$ to 0.0045 $mm^3$ in BkF-exposed embryos. There were no significant differences in ventricular diameter or contractility between either BaP- or BkF-exposed embryos and controls. Because the ventricular stroke volume was the same in BkF-exposed embryos and controls, BkF-induced bradycardia resulted in a 22% reduction of cardiac output. Embryos exposed to either BaP or BkF but not BeP frequently had intracranial hemorrhages (e.g., arrow in Fig. 1B), but this was not quantified. The toxicity of the mixtures was not significantly different than individual compounds. However, the mixtures included either 20 μM or 13 μM of each compound in binary or ternary combinations, respectively, and a simple additive toxicity model would predict a severity of edema intermediate to BaP or BkF alone.

### *Benzo[a]pyrene, benzo[e]pyrene, and benzo[k]fluoranthene induce CYP1A in distinct tissue-specific patterns*

Because all three PAHs are known to have AHR binding activity, we assessed the distribution of CYP1A induction after exposure to relate tissue-specific AHR activation to toxic effects. BaP, BeP, and BkF exposures each resulted in a distinct pattern of CYP1A induction that partially overlapped (Fig. 2). BaP exposure resulted in CYP1A immunofluorescence throughout the epidermis (apparent on the head, Fig. 2A, and dorsal finfold, Fig. 2B) and vascular endothelium of the head and trunk (Fig. 2A–C). The level of CYP1A signal in the epidermis was relatively low, allowing the visualization of vascular CYP1A through the epidermis. BaP exposure also resulted in the induction of CYP1A immunofluorescence in the urinary pore and liver bud (Fig. 2C, inset). BeP exposure resulted in a lower level of CYP1A immunofluorescence in the vascular endothelium of the head and trunk, with induction in a few epidermal cells scattered over the eye (Fig. 2D–F). In striking contrast to BaP and BeP, exposure to BkF resulted in a very strong induction of CYP1A immunofluorescence in the epidermis only (Fig. 2G–I). Optical sections showed robust detection of the *fli1*GFP endothelial marker and the absence of vascular endothelial CYP1A (Fig. 2H, I). Examination of at least 20 embryos showed that there was a very weak vascular CYP1A signal in about 10% of BkF-exposed embryos (see below), while all showed strong epidermal induction.

A close examination of the heart also showed marked differences between BaP and BkF (Fig. 3). BaP exposure induced CYP1A immunofluorescence in both the endocardium (Fig. 3A, arrows) and in a subset of myocardial cells (Fig. 3A, arrowheads). Consistent with the absence of vascular endothelial CYP1A induction in response to BkF treatment, CYP1A immunofluorescence was generally absent in endocardial cells, but was also absent in the myocardium (Fig. 3B). About 1 in 10 BkF-exposed embryos showed weak endocardial CYP1A induction (e.g., Fig. 5).

### *Cardiac toxicity of benzo[a]pyrene but not benzo[k]fluoranthene is AHR2-dependent*

The severity of pericardial edema at 48 hpf was used to determine whether knockdown of the AHR2 isoform modulates the toxicity of BaP and BkF. Consistent with previous studies, injection of either the standard control morpholino (std-MO) or *ahr2* morpholino (*ahr2*-MO) followed by exposure to solvent (DMSO) did not result in a significant increase in pericardial edema (Fig. 4A). As a positive control, embryos injected with either std-MO or *ahr2*-MO were exposed to BaA, which has been previously shown to produce AHR2-dependent pericardial edema (Incardona et al., 2006). In this case *ahr2* morphants exposed to

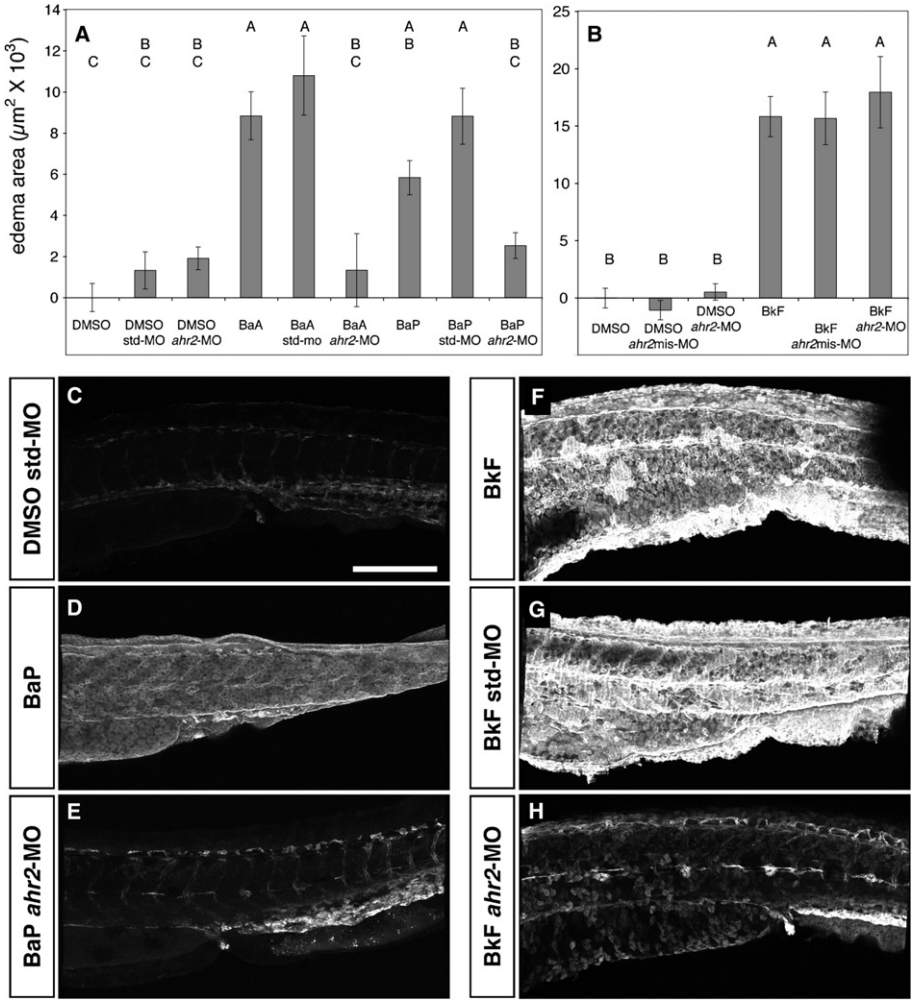


**Fig. 4.** Effects of AHR2 knockdown on PAH toxicity and tissue-specific patterns of CYP1A induction. Uninjected embryos or embryos injected with control or *ahr2* MOs were exposed to (A) indicated PAHs or DMSO alone or (B) BkF or DMSO alone from 4 to 48 hpf and pericardial area was measured in lateral images as described in the Materials and methods. Data were derived from 17 to 25 embryos per treatment group, with values for BaA and BaP pooled from two experiments, and values for BkF from a one of three experiments (see text). Control-MO was standard-MO for BaA and BaP, and 4-mis*Ahr2*-MO for BkF. Data were analyzed by one-way ANOVA ($p<0.0001$) with post-hoc means comparisons using Tukey–Kramer HSD test (alpha = 0.05). Letters (A, B, C) indicate statistically similar groups in post-hoc tests. (C–H) Representative lateral confocal stack projections showing CYP1A immunofluorescence in the trunk region, with anterior at left and dorsal at top. (C) Standard control-MO-injected exposed to DMSO, (D) uninjected exposed to BaP, (E) *ahr2*-MO-injected exposed to BaP, (F) uninjected exposed to BkF, (G) standard control-MO-injected exposed to BkF, (H) *ahr2*-MO-injected exposed to BkF.

BAA had an average pericardial area indistinguishable from DMSO-exposed controls, while the std-MO had no effect on BAA-induced pericardial edema (Fig. 4A). In contrast, AHR2 knockdown only partially protected from BaP toxicity (Fig. 4A). Although *ahr2* morphants exposed to BaP had a significant reduction in edema compared to std-MO-injected embryos exposed to BaP, they retained a measurable degree of edema that was not significantly lower than uninjected BaP-exposed embryos. In contrast to BaA and BaP, edema associated with BkF exposure was completely resistant to AHR2 knockdown (Fig. 4B). In three experiments, BkF-exposed *ahr2* morphants had no significant reduction in edema compared to uninjected BkF-exposed embryos, but embryos injected with standard control morpholino had an increased sensitivity to BkF, showing much more severe edema (see below, Fig. 6). Therefore, we assessed BkF dependency on AHR2 function in a fourth experiment using the *ahr2* mismatch control morpholino (Fig. 4B). In this case, embryos injected with the *ahr2* mismatch control morpholino had a similar response to BkF exposure as uninjected embryos (Fig. 4B), and again, there was no effect of AHR2 knockdown.

We examined the distribution of CYP1A immunofluorescence after AHR2 knockdown (Fig. 4C–H). Control embryos exposed to DMSO showed low levels of CYP1A immunofluorescence in the vasculature (Fig. 4C). As we observed previously with some other PAHs, AHR2 knockdown resulted primarily in loss of epidermal but not vascular CYP1A induction in embryos exposed to either BaP or BkF (Fig. 4D, E and F, H). Although embryos injected with standard control morpholino were more sensitive to BkF toxicity, there was no effect on CYP1A induction (Fig. 4G). Consistent with partial protection from BaP cardiotoxicity, AHR2 knockdown resulted in a loss of myocardial CYP1A immunofluorescence, while CYP1A+ endocardial cells were still detected (Fig. 5A, B). AHR2 knockdown markedly reduced the epidermal induction of CYP1A by BkF, but did not influence the variable endocardial CYP1A induction observed in BkF-exposed embryos (Fig. 5C, D).

We explored a potential role for AHR2 in BkF toxicity further by testing the sensitivity of lower BkF doses to modulation by AHR2 knockdown. In addition, we tested whether CYP1A is protective of or contributes to BkF toxicity. Uninjected embryos or embryos injected with standard control, *ahr2*, or *cyp1a* morpholinos were exposed to BkF at concentrations ranging from 4 to 40 μM (Fig. 6). Although there was no significant difference from uninjected controls in the severity of edema for *ahr2* morphants at any dose, the severity of edema was significantly higher for *cyp1a* morphants at each dose except the highest. Embryos injected with the standard control morpholino were more sensitive to BkF exposure, showing an increased severity of edema.

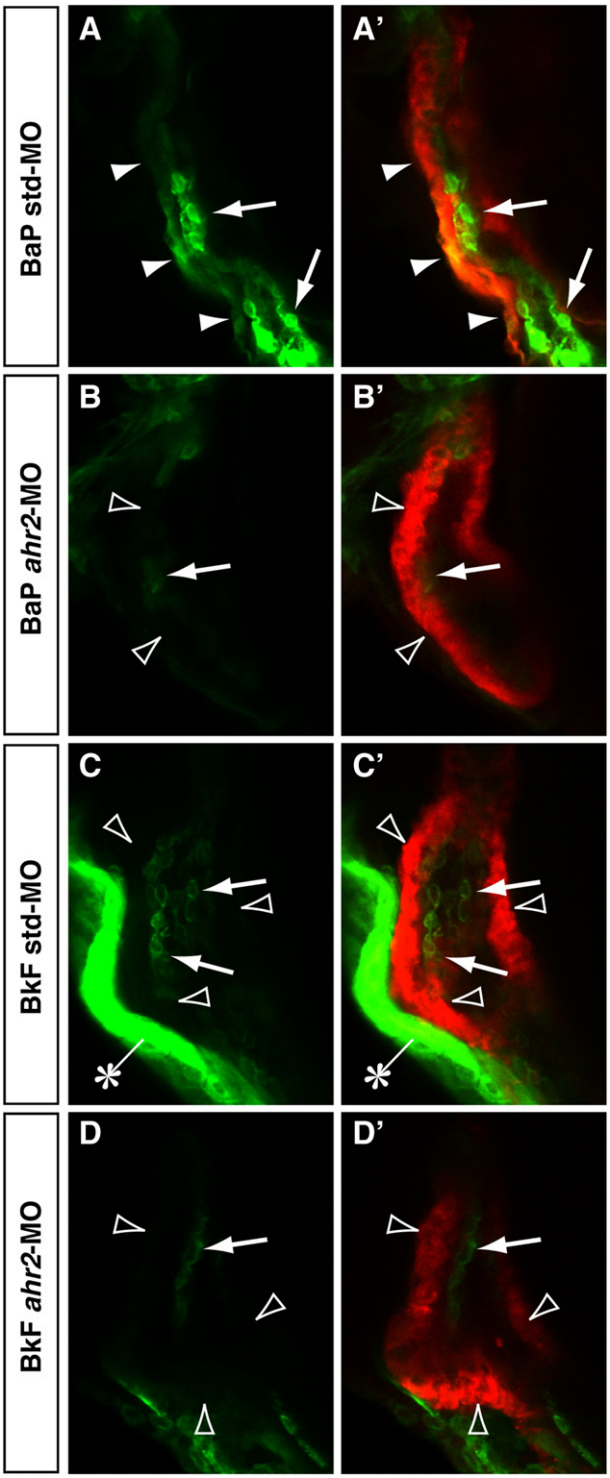


**Fig. 5.** Prevention of BaP cardiotoxicity by AHR2 knockdown also reduces myocardial CYP1A induction. Wild type embryos were injected with morpholinos then exposed to BaP or BkF from 4 to 48 hpf, fixed and processed for CYP1A (green) and myosin heavy chain (red) immunofluorescence as described in the Materials and methods. Left panels show CYP1A and right panels show CYP1A/myosin heavy chain merged image, with co-localization appearing yellow. (A, A′) CYP1A immunofluorescence in the myocardium (filled arrowheads) and endocardium (arrows) of an embryo injected with standard control morpholino and exposed to BaP. (B, B′) CYP1A-negative myocardium (unfilled arrowheads) and weakly positive endocardial CYP1A (arrows) in an *ahr2* morphant exposed to BaP. (C, C′) CYP1A-negative myocardium (unfilled arrowheads), weakly positive endocardial CYP1A (arrows), and strongly positive epidermal CYP1A (asterisk) in an embryo injected with standard control morpholino and exposed to BkF. (D, D′) CYP1A-negative myocardium (unfilled arrowheads) and weakly positive endocardial CYP1A (arrows) in an *ahr2* morphant exposed to BkF.

## Discussion

While we have not tested PAH compounds at environmentally typical concentrations, our goal was to use a screening approach in zebrafish to identify potential pathways by which these compounds may affect early life history stages of fish. Past studies on low molecular weight (3-ring) PAHs demonstrate how this screening approach provided insight into the mechanisms underlying the toxicity of very low concentrations of crude oil in zebrafish (Hicken et al., 2011; Incardona et al., 2004, 2005), as well as non-model species of ecological importance (Incardona et al., 2009). The findings presented here provide further evidence that individual PAH compounds have the capacity to act through distinct toxic mechanisms, even among the subgroup that target the cardiovascular system. Most high molecular weight PAH compounds are relatively strong AHR ligands, and are assumed to act in an AHR-dependent manner. This includes, for example, the 4-ring compound benz[a]anthracene (BaA). Similar to dioxin (TCDD: (Antkiewicz et al., 2005), BaA has no effect on heart rate, produces morphological defects (reduced ventricular cardiomyocyte proliferation) relatively late in embryonic stages of heart development, and activates AHR strongly in embryonic ventricular myocardium (as measured by CYP1A induction). Each of these effects are completely prevented by AHR2 knockdown (Incardona et al., 2006). At lower concentrations than we used here (e.g., 0.04–0.4 μM), BaP alone did not cause pericardial edema or other cardiac defects in either zebrafish or *Fundulus heteroclitus* embryos, but pharmacological inhibition of CYP1A markedly increased the occurrence of BaP-induced cardiac defects in both species (Matson et al., 2008; Wills et al., 2009). In many respects, BaP (at higher concentrations) acts in a manner similar to BaA in zebrafish embryos. Although both BaA and BaP are predicted to have similar potency as AHR agonists (Barron et al., 2004), BaP was less potent than BaA in terms of causing cardiac defects and inducing myocardial CYP1A in zebrafish embryos. BaP also acts somewhat differently than BaA in that it caused a slight bradycardia, and protection provided by AHR2 knockdown was not as robust. Nevertheless, the primary mode of action for BaP in zebrafish embryos is AHR2-dependent cardiotoxicity. The differences between the very strict AHR2-dependency of BaA and the partial dependency observed with BaP could reflect differences in the role of metabolism or specific metabolites in BaP cardiotoxicity. If BaP metabolites contributed to toxicity, it is possible that some toxicity is retained in *ahr2* morphants due to the refractory CYP1A induction, or other CYP1 family members that are AHR2 targets (e.g. CYP1B and CYP1C isoforms (Jönsson et al., 2007)). Similarly, zebrafish embryos express a higher basal level of CYP1D1 that most likely has the ability to metabolize BaP (Goldstone et al., 2009). Future studies should focus on these additional enzymes, but would require more complicated multiple knockdown experiments.

The toxicity of BkF is more complicated. In *Fundulus heteroclitus* embryos, BkF produced cardiac defects at 1.2 μM that were prevented by knockdown of the *Fundulus* AHR2 ortholog, but not by knockdown of the AHR1 ortholog (Clark et al., 2010). However, cardiac dysfunction or dysmorphogenesis were not described in this recent study, nor was there an assessment of the tissue specificity of AHR activation. Our findings indicate a different mode of action for BkF-induced cardiotoxicity in zebrafish embryos that is unlike any other PAH studied in the zebrafish model to date. Specifically, BkF causes cardiac dysfunction without myocardial AHR activation that is measurable by CYP1A induction, and without consistent endocardial CYP1A induction. Moreover, BkF-induced cardiotoxicity is not modulated significantly by AHR2 knockdown. Although CYP1A appears to be partially protective for BkF toxicity, as is the case for BaP, future studies could focus on a role for metabolites generated by other CYP family members. For example, it is conceivable that loss of CYP1A activity could provide more substrate for other CYP family members to produce toxic metabolites.

So far, three PAH compounds have been identified that cause true dioxin-like, AHR2-dependent cardiotoxicity in zebrafish: BaA, BaP, and retene. For each compound, cardiac defects are associated with

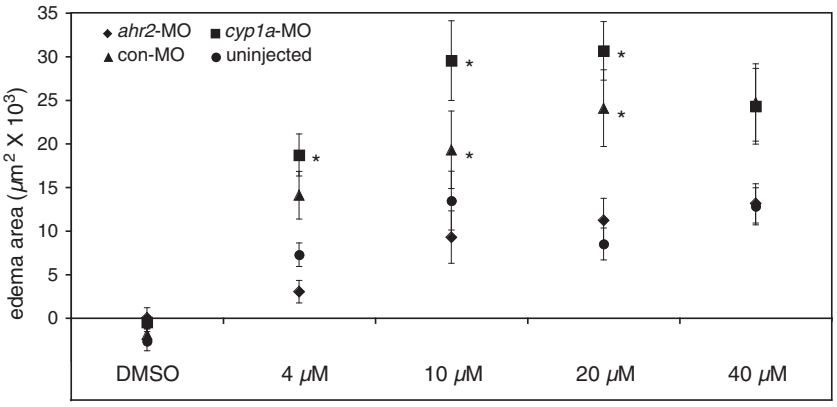


**Fig. 6.** BkF cardiotoxicity is AHR2- and CYP1A-independent across a range of doses. Uninjected embryos and embryos injected with the indicated morpholinos were exposed to BkF at 4–40 μM to 48 hpf, and then pericardial edema was quantified as increased pericardial area in lateral images. Data represent a single experiment with 14 or 15 embryos per treatment group (mean ± s.e.m.). Asterisks indicate treatment groups significantly different from uninjected controls as described in the text (ANOVA with Tukey–Kramer HSD ($\alpha = 0.05$).

myocardial AHR activation (indicated by CYP1A induction), which is simply blocked by AHR2 knockdown, restoring normal cardiac morphogenesis (Incardona et al., 2006; Scott et al., 2011). By contrast, it is difficult to reconcile the pattern of CYP1A induction resulting from BkF exposure, the effects of AHR2 knockdown on that pattern, and the impacts of BkF exposure on heart function. Consistent with predictions based on AHR agonist activity in cell lines (Barron et al., 2004), BkF is a strong inducer in zebrafish, causing qualitatively much higher levels of AHR2-dependent epidermal CYP1A immunofluorescence than BaP. If BkF acts directly on the myocardium to reduce heart rate and cause atrial dilation, it does so without evidence of AHR activation in target cardiac cells. It is possible that BkF acts on myocardial cells through one of the other zebrafish AHR orthologs (AHR1A and AHR1B), independent of CYP1A induction. This is highly unlikely, as *cyp1a* is consistently the most highly induced gene following AHR activation (Alexeyenko et al., 2010; Carney et al., 2006). There is no simple mechanism to explain how BkF could induce CYP1A in an AHR2-dependent manner in epidermal cells, but fail to induce CYP1A in myocardial cells.

An alternative explanation is that cardiac toxicity in BkF-exposed embryos is a result of a metabolite of BkF, or another metabolic alteration resulting from BkF exposure. BkF toxicity was moderately increased by CYP1A knockdown, which could indicate either that the parent compound causes toxicity, or that more parent compound is accessible to another metabolic pathway. The interaction between BkF and the standard control morpholino is unusual and also could implicate a metabolic mechanism. The standard control morpholino targets a splice site in the human ß-globin gene, has no antisense activity in zebrafish cells, and was selected for its absence of off-target biological activity or toxicity (Lacerra et al., 2000) (http://www.gene-tools.com/node/23#standardcontrols). Some morpholinos have been shown to produce off-target toxicity causing apoptotic cell death through the p53 pathway (Robu et al., 2007). We have used the standard control morpholino with several other PAHs, and have not observed a similarly increased sensitivity to PAH toxicity (Incardona et al., 2006). There are no similar published findings that may suggest a plausible hypothesis underlying this effect. A BLAST search against the current zebrafish genome database with this sequence reveals only two anonymous sequences that have a partial (19 base pair) overlap with the morpholino target sequence. Therefore, the control morpholino cannot be targeting a known member of the AHR or cytochrome P450 family. The observed synergism cannot be due to a general metabolic property of morpholinos, because the effect was sequence-specific, i.e. did not occur with either the *ahr2*-specific negative control morpholino, or the *ahr2* antisense morpholino.

The PAH compositions derived from non-point sources such as stormwater runoff are complex and typically reflect a mixture of combustive and petrogenic sources (Hwang and Foster, 2006; Stein et al., 2006). Comparison of dissolved-phase and particulate-associated PAHs usually shows a predominance of 2- and 3-ring compounds in the dissolved phase, with a predominance of 4-, 5-, and 6-ring compounds in the particulate fraction. While the bulk of larger particle-associated PAHs may not be bioavailable to organisms such as fish embryos that are primarily impacted by dissolved PAHs (Carls et al., 2008), a key question is how lower concentrations of compounds such as BaP and BkF might modify the toxicity of a mixture that is otherwise predominantly petrogenic. Because CYP1A induction is primarily protective against petrogenic PAH toxicity (Hicken et al., 2011; Incardona et al., 2005), the presence of low concentrations of potent CYP1A inducers could potentially reduce the effects of 3-ring compounds in a mixture. Alternatively, if CYP1A metabolic capacity was already overwhelmed by higher concentrations of low molecular weight PAHs (which occurs at about 10 μg/L in zebrafish; (Hicken et al., 2011), the high molecular weight compounds may produce additive or greater-than-additive (i.e., synergistic) impacts on cardiac function and morphogenesis. The finding that the various mixtures of BeP, BaP, and BkF did not produce intermediate levels of toxicity suggests that there may be more complicated interactions between these compounds, which should be examined in more detailed studies.

In conclusion, these findings refine and extend our understanding of how individual PAHs cause developmental toxicity via a diversity of toxicokinetic and toxicodynamic processes. This understanding is critical for assessing the combinatorial toxicity of PAH mixtures in aquatic habitats, both within and between petrogenic and pyrogenic sources. There are numerous implications for improving environmental assessment in PAH-contaminated environments. This includes, for example, future assessments of oil spill impacts (primarily petrogenic PAH mixtures) in riverine, estuarine, or coastal marine habitats where inputs from urban stormwater runoff (primarily pyrogenic mixtures) are common. A long-term goal of this work is to develop mechanism-based markers of the biological effects of complex PAH mixtures in sensitive early life history stages of fish. This goal is dependent on a detailed understanding of the various pathways through which PAH toxicity converges on the developing fish heart. Although the results of our zebrafish screening approach with high concentrations of single compounds may not be environmentally relevant, they shed light on pathways (e.g. AHR-dependent and novel AHR-independent) for which gene expression markers can be developed and tested with real-world mixtures. These types of mechanistic analyses using the zebrafish model will ultimately inform the development of a new generation of biomarkers that will be diagnostic of different types of PAH exposures in fish spawning habitats and, at the same time, phenotypically anchored to cardiac performance, heart and vascular development, and fish survival.

Supplementary material related to this article can be found online at doi:10.1016/j.taap.2011.09.010.

## Conflict of interest statement

All authors declare no conflict of interest.

## Acknowledgments

This project was funded in part by the NOAA Coastal Storms Program, the NOAA Oceans and Human Health Initiative, and the Regional Monitoring Program for Water Quality in the San Francisco Estuary (RMP), which is managed by the San Francisco Estuary Institute, Oakland, CA. No funding source was involved in the design or implementation of the studies described herein.

## References

Alexeyenko, A., Wassenberg, D.M., Lobenhofer, E.K., Yen, J., Linney, E., Sonnhammer, E.L., Meyer, J.N., 2010. Dynamic zebrafish interactome reveals transcriptional mechanisms of dioxin toxicity. PLoS One 5, e10465.

Andreasen, E.A., Hahn, M.E., Heideman, W., Peterson, R.E., Tanguay, R.L., 2002a. The zebrafish (*Danio rerio*) aryl hydrocarbon receptor type 1 is a novel vertebrate receptor. Mol. Pharmacol. 62, 234–249.

Andreasen, E.A., Spitsbergen, J.M., Tanguay, R.L., Stegeman, J.J., Heideman, W., Peterson, R.E., 2002b. Tissue-specific expression of AHR2, ARNT2, and CYP1A in zebrafish embryos and larvae: effects of developmental stage and 2,3,7,8-tetrachlorodibenzo-p-dioxin exposure. Toxicol. Sci. 68, 403–419.

Antkiewicz, D.S., Burns, C.G., Carney, S.A., Peterson, R.E., Heideman, W., 2005. Heart malformation is an early response to TCDD in embryonic zebrafish. Toxicol. Sci. 84, 368–377.

Bader, D., Masaki, T., Fischman, D.A., 1982. Immunochemical analysis of myosin heavy chain during avian myogenesis in vivo and in vitro. J. Cell Biol. 95, 763–770.

Barron, M.G., Heintz, R.A., Rice, S.D., 2004. Relative potency of PAHs and heterocycles as aryl hydrocarbon receptor agonists in fish. Mar. Environ. Res. 58, 95–100.

Bendig, G., Grimmler, M., Huttner, I.G., Wessels, G., Dahme, T., Just, S., Trano, N., Katus, H.A., Fishman, M.C., Rottbauer, W., 2006. Integrin-linked kinase, a novel component of the cardiac mechanical stretch sensor, controls contractility in the zebrafish heart. Genes Dev. 20, 2361–2372.

Billiard, S.M., Timme-Laragy, A.R., Wassenberg, D.M., Cockman, C., Di Giulio, R.T., 2006. The role of the aryl hydrocarbon receptor pathway in mediating synergistic developmental toxicity of polycyclic aromatic hydrocarbons to zebrafish. Toxicol. Sci. 92, 526–536.

Billiard, S.M., Meyer, J.N., Wassenberg, D.M., Hodson, P.V., Di Giulio, R.T., 2008. Nonadditive effects of PAHs on Early Vertebrate Development: mechanisms and implications for risk assessment. Toxicol. Sci. 105, 5–23.

Carls, M.G., Rice, S.D., Hose, J.E., 1999. Sensitivity of fish embryos to weathered crude oil: Part I. Low-level exposure during incubation causes malformations, genetic damage, and mortality in larval Pacific herring (*Clupea pallasi*). Environ. Toxicol. Chem. 18, 481–493.

Carls, M.G., Holland, L., Larsen, M., Collier, T.K., Scholz, N.L., Incardona, J.P., 2008. Fish embryos are damaged by dissolved PAHs, not oil particles. Aquat. Toxicol. 88, 121–127.

Carney, S.A., Peterson, R.E., Heideman, W., 2004. 2,3,7,8-Tetrachlorodibenzo-p-dioxin activation of the aryl hydrocarbon receptor/aryl hydrocarbon receptor nuclear translocator pathway causes developmental toxicity through a CYP1A-independent mechanism in zebrafish. Mol. Pharmacol. 66, 512–521.

Carney, S.A., Chen, J., Burns, C.G., Xiong, K.M., Peterson, R.E., Heideman, W., 2006. Aryl hydrocarbon receptor activation produces heart-specific transcriptional and toxic responses in developing zebrafish. Mol. Pharmacol. 70, 549–561.

Clark, B.W., Matson, C.W., Jung, D., Di Giulio, R.T., 2010. AHR2 mediates cardiac teratogenesis of polycyclic aromatic hydrocarbons and PCB-126 in Atlantic killifish (*Fundulus heteroclitus*). Aquat. Toxicol. 99, 232–240.

Colavecchia, M.V., Backus, S.M., Hodson, P.V., Parrott, J.L., 2004. Toxicity of oil sands to early life stages of fathead minnows (*Pimephales promelas*). Environ. Toxicol. Chem. 23, 1709–1718.

Couillard, C.M., 2002. A microscale test to measure petroleum oil toxicity to mummichog embryos. Environ. Toxicol. 17, 195–202.

Goldstone, J.V., J˜nsson, M.E., Behrendt, L., Woodin, B.R., Jenny, M.J., Nelson, D.R., Stegeman, J.J., 2009. Cytochrome P450 1D1: a novel CYP1A-related gene that is not transcriptionally activated by PCB126 or TCDD. Arch. Biochem. Biophys. 482, 7–16.

Hahn, M.E., 2002. Aryl hydrocarbon receptors: diversity and evolution. Chem. Biol. Interact. 141, 131–160.

Heintz, R.A., Short, J.W., Rice, S.D., 1999. Sensitivity of fish embryos to weathered crude oil: Part II. Increased mortality of pink salmon (*Oncorhynchus gorbuscha*) embryos incubating downstream from weathered Exxon Valdez crude oil. Environ. Toxicol. Chem. 18, 494–503.

Heintz, R.A., Rice, S.D., Wertheimer, A.C., Bradshaw, R.F., Thrower, F.P., Joyce, J.E., Short, J.W., 2000. Delayed effects on growth and marine survival of pink salmon *Oncorhynchus gorbuscha* after exposure to crude oil during embryonic development. Mar. Ecol. Prog. Ser. 208, 205–216.

Henry, T.R., Spitsbergen, J.M., Hornung, M.W., Abnet, C.C., Peterson, R.E., 1997. Early life stage toxicity of 2,3,7,8-tetrachlorodibenzo-p-dioxin in zebrafish (*Danio rerio*). Toxicol. Appl. Pharmacol. 142, 56–68.

Hicken, C.E., Linbo, T.L., Baldwin, D.H., Myers, M.S., Holland, L., Larsen, M., Scholz, N.L., Collier, T.K., Rice, G.S., Stekoll, M.S., Incardona, J.P., 2011. Sub-lethal exposure to crude oil during embryonic development alters cardiac morphology and reduces aerobic capacity in adult fish. Proc. Natl. Acad. Sci. U. S. A. 108, 7086–7090.

Hwang, H.M., Foster, G.D., 2006. Characterization of polycyclic aromatic hydrocarbons in urban stormwater runoff flowing into the tidal Anacostia River, Washington, DC, USA. Environ. Pollut. 140, 416–426.

Incardona, J.P., Collier, T.K., Scholz, N.L., 2004. Defects in cardiac function precede morphological abnormalities in fish embryos exposed to polycyclic aromatic hydrocarbons. Toxicol. Appl. Pharmacol. 196, 191–205.

Incardona, J.P., Carls, M.G., Teraoka, H., Sloan, C.A., Collier, T.K., Scholz, N.L., 2005. Aryl hydrocarbon receptor-independent toxicity of weathered crude oil during fish development. Environ. Health Perspect. 113, 1755–1762.

Incardona, J.P., Day, H.L., Collier, T.K., Scholz, N.L., 2006. Developmental toxicity of 4-ring polycyclic aromatic hydrocarbons in zebrafish is differentially dependent on AH receptor isoforms and hepatic cytochrome P450 1A metabolism. Toxicol. Appl. Pharmacol. 217, 308–321.

Incardona, J.P., Carls, M.G., Day, H.L., Sloan, C.A., Bolton, J.L., Collier, T.K., Scholz, N.L., 2009. Cardiac arrhythmia is the primary response of embryonic Pacific herring (*Clupea pallasi*) exposed to crude oil during weathering. Environ. Sci. Technol. 43, 201–207.

Incardona, J.P., Collier, T.K., Scholz, N.L., 2011. Oil spills and fish health: exposing the heart of the matter. J. Expo. Sci. Environ. Epidemiol. 21, 3–4.

Jönsson, M.E., Jenny, M.J., Woodin, B.R., Hahn, M.E., Stegeman, J.J., 2007. Role of AHR2 in the expression of novel cytochrome P450 1 family genes, cell cycle genes, and morphological defects in developing zebra fish exposed to 3,3,Ä≤,4,4,Ä≤,5-pentachlorobiphenyl or 2,3,7,8-tetrachlorodibenzo-p-dioxin. Toxicol. Sci. 100, 180–193.

Karchner, S.I., Franks, D.G., Hahn, M.E., 2005. AHR1B, a new functional aryl hydrocarbon receptor in zebrafish: tandem arrangement of ahr1b and ahr2 genes. Biochem. J. 392.

Kimbrough, K.L., Dickhut, R.M., 2006. Assessment of polycyclic aromatic hydrocarbon input to urban wetlands in relation to adjacent land use. Mar. Pollut. Bull. 52, 1355–1363.

Kopp, R., Schwerte, T., Pelster, B., 2005. Cardiac performance in the zebrafish breakdance mutant. J. Exp. Biol. 208, 2123–2134.

Lacerra, G., Sierakowska, H., Carestia, C., Fucharoen, S., Summerton, J., Weller, D., Kole, R., 2000. Restoration of hemoglobin A synthesis in erythroid cells from peripheral blood of thalassemic patients. Proc. Natl. Acad. Sci. U. S. A. 97, 9591–9596.

Lawson, N.D., Weinstein, B.M., 2002. In vivo imaging of embryonic vascular development using transgenic zebrafish. Dev. Biol. 248, 307–318.

Linbo, T.L., 2009. Zebrafish (*Danio rerio*) husbandry and colony maintenance at the Northwest Fisheries Science Center. NOAA Technical Memorandum. U. S. Department of Commerce, p. 75.

Matson, C.W., Timme-Laragy, A.R., Di Giulio, R.T., 2008. Fluoranthene, but not benzo[a] pyrene, interacts with hypoxia resulting in pericardial effusion and lordosis in developing zebrafish. Chemosphere 74, 149–154.

Myers, C.R., Sutherland, L.A., Haasch, M.L., Lech, J.J., 1993. Antibodies to a synthetic peptide that react specifically with rainbow-trout hepatic cytochrome-P450 1a1. Environ. Toxicol. Chem. 12, 1619–1626.

Nebert, D.W., Dalton, T.P., Okey, A.B., Gonzalez, F.J., 2004. Role of aryl hydrocarbon receptor-mediated induction of the CYP1 enzymes in environmental toxicity and cancer. J. Biol. Chem. 279, 23847–23850.

Robu, M.E., Larson, J.D., Nasevicius, A., Beiraghi, S., Brenner, C., Farber, S.A., Ekker, S.C., 2007. p53 activation by knockdown technologies. PLoS Genet. 3, e78.

Scott, J.A., Incardona, J.P., Pelkki, K., Shepardson, S., Hodson, P.V., 2011. AhR2-mediated; CYP1A-independent cardiovascular toxicity in zebrafish (*Danio rerio*) embryos exposed to retene. Aquat. Toxicol. 101, 165–174.

Stein, E.D., Tiefenthaler, L.L., Schiff, K., 2006. Watershed-based sources of polycyclic aromatic hydrocarbons in urban storm water. Environ. Toxicol. Chem. 25, 373–385.

Sundberg, H., Ishaq, R., Akerman, G., Tjarnlund, U., Zebuhr, Y., Linderoth, M., Broman, D., Balk, L., 2005. A bio-effect directed fractionation study for toxicological and chemical characterization of organic compounds in bottom sediment. Toxicol. Sci. 84, 63–72.

Tanguay, R.L., Abnet, C.C., Heideman, W., Peterson, R.E., 1999. Cloning and characterization of the zebrafish (*Danio rerio*) aryl hydrocarbon receptor. Biochim. Biophys. Acta 1444, 35–48.

Teraoka, H., Dong, W., Tsujimoto, Y., Iwasa, H., Endoh, D., Ueno, N., Stegeman, J.J., Peterson, R.E., Hiraga, T., 2003. Induction of cytochrome P450 1A is required for circulation failure and edema by 2,3,7,8-tetrachlorodibenzo-p-dioxin in zebrafish. Biochem. Biophys. Res. Commun. 304, 223–228.

Vines, C.A., Robbins, T., Griffin, F.J., Cherr, G.N., 2000. The effects of diffusible creosote-derived compounds on development in Pacific herring (*Clupea pallasi*). Aquat. Toxicol. 51, 225–239.

Wills, L.P., Zhu, S., Willett, K.L., Di Giulio, R.T., 2009. Effect of CYP1A inhibition on the biotransformation of benzo[a]pyrene in two populations of *Fundulus heteroclitus* with different exposure histories. Aquat. Toxicol. 92, 195–201.